Eur. Phys. J. Special Topics **172**, 297–309 (2009)
© EDP Sciences, Springer-Verlag 2009
DOI: 10.1140/epjst/e2009-01055-1

THE EUROPEAN PHYSICAL JOURNAL SPECIAL TOPICS

Review

Practical aspects of counting electrons with a single-electron tunneling pump[⋆]

M.W. Keller[a]

National Institute of Standards and Technology (NIST), 325 Broadway, Boulder, CO 80305-3328, USA

Abstract. This review covers various aspects of the single-electron tunneling pumps based on Al junctions studied at NIST over the past 15 years. The operation of a pump is described, and some important error mechanisms are summarized, which allows for a sketch of the basic pump parameters required for metrological accuracy. Fabrication of pumps, filtering of leads in the cryostat, and the electronics used to drive the pump are described next. The shuttle error technique that allows measurement of very rare errors is then described, and some outstanding questions about limitations of pumps based on Al junctions are mentioned. A detailed algorithm for cancelling the cross capacitance in a pump is described in an appendix.

1 Introduction

The transfer of individual electrons controlled by an external signal was first demonstrated by Pothier et al. in 1991 in a single-electron tunneling (SET) pump with 3 aluminum junctions [1]. The current produced by this device was within 1 part in 10^3 of the nominal value $I = ef$, where e is the elementary charge and f is the pumping frequency. Similar pumps with 5 junctions [2] and 7 junctions [3] were made at NIST and shown to have an error per cycle of about 5 parts in 10^6 and 1 part in 10^8, respectively. In these devices, each electron transfer event could be monitored by a nearby SET transistor, thus the pumped electrons could literally be "counted". The 7-junction pump was good enough for use in fundamental metrology, in particular for a standard of capacitance based on counting electrons [4]. Such a standard was first demonstrated in 1998 [5], and a full uncertainty budget has recently been completed [6]. Rather than pushing for lower error rates, efforts over the last 10 years have focused on (1) understanding the large discrepancy between theory and experiment for the error rate [7–10], (2) quantifying the limitations on pump performance when it is used for a capacitance standard [11], and (3) simplifying pump operation by achieving the same error rate with fewer junctions [12,13]. In addition, several other types of devices that can produce a current by transferring individual electrons (or Cooper pairs in the superconducting state) have been explored. A broad (but somewhat dated) review of these approaches can be found in [14]. See the article by Kemppinen et al. in this book [15] for recent references and a detailed discussion of a new scheme of this type. In general, these approaches promise much larger current than is possible with an SET pump but have yet to demonstrate the accuracy needed for metrology.

This article begins with a review of SET pump operation and error mechanisms, and then discusses several practical aspects of using SET pumps. The aim is to give the reader a sense for the main challenges in implementing an SET pump in a metrology experiment and to

[⋆] Official contribution of the National Institute of Standards and Technology; not subject to copyright in the United States.

[a] e-mail: mark.keller@boulder.nist.gov

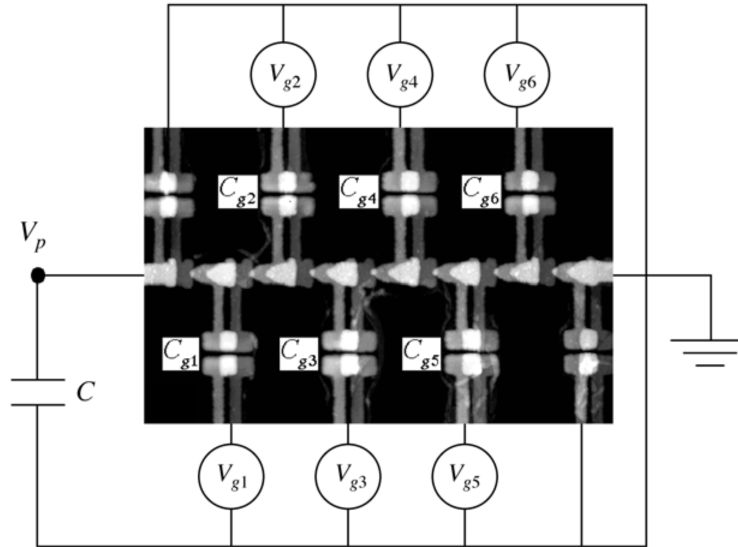

Fig. 1. A 7-junction SET pump. The center part is a scanning force microscope image of an actual device. (There is an extra gate structure at each end to ensure that proximity effects during lithography are the same for all junctions.) External connections are drawn for the case when the pump is used to place a known number of electrons on an external capacitance C. When the pump is used as a current source, the capacitance is usually replaced by an ammeter that fixes $V_{\mathrm{p}} \approx 0$.

describe various limitations on pump performance that have been measured. Although some of this material appeared in a previous paper [16], experts will find several new details about the NIST pumps.

2 Review of conventional SET pump

The SET pump consists of a chain of μm-sized metal islands separated by nanoscale tunnel junctions, with a gate electrode coupled capacitively to each island. Figure 1 shows a composite view of the pump itself and the external gate sources. (Cross capacitance between neighboring gates is ignored for the moment; it is considered in detail in section 5.) A sequence of gate voltage pulses that transfers an electron through a 4-junction pump is shown in figure 2. Tunneling at a given junction is allowed for a time t_{j} during which the corresponding gate is biased above the threshold $C_{\mathrm{g}}V_{\mathrm{g}} = e/2$. One can think of the gate sources as creating a positive charge polarization that moves along the chain of junctions and induces a single electron to follow it. Additional electrons are excluded by the Coulomb repulsion energy, which is of order $e^2/(2C_{\mathrm{tot}})$, where C_{tot} is the total capacitance of one island. The direction of electron transfer is determined simply by the order in which the gates are pulsed.

The schematic energy diagram in figure 3 illustrates three error mechanisms that can interfere with the desired transfer of a single electron in one cycle of the pump. The short horizontal lines are the electrostatic energy of the system as a function of the location of one extra electron in the pump, and they are drawn for a point during the pumping cycle where the first island is biased to allow tunneling across the first junction. (Similar diagrams for an entire cycle can be found in figure 3 of [11].) The desired process at this point in the cycle is tunneling from island 0 to island 1, and one can identify three unwanted processes that will result in an error:

1. *Switching errors (failure to tunnel).* Once the threshold for tunneling is passed, the probability that the electron has not tunneled decreases according to a Poisson distribution with a characteristic time of order $R_{\mathrm{j}}C_{\mathrm{j}}$, where R_{j} is the junction resistance and C_{j} is the junction capacitance. This process, which is represented by a dashed arrow in figure 3, leads to an

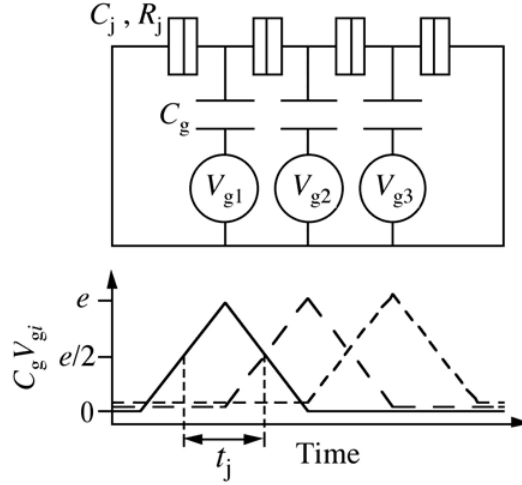

Fig. 2. Schematic plot of gate voltage pulses that transfer one electron through a 4-junction pump. Solid line is gate 1, long dashed line is gate 2, short dashed line is gate 3, and the traces are offset vertically for clarity. Tunneling is allowed at each junction during a time t_{j}.

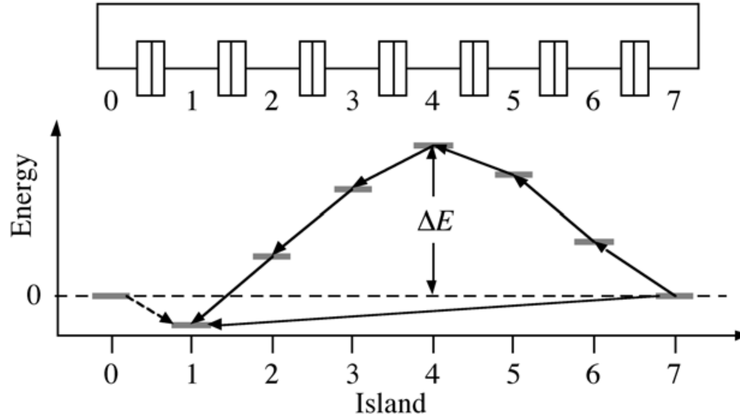

Fig. 3. Schematic plot of electrostatic energy (short gray lines) *vs.* position of one extra electron in a 7-junction pump. The different arrows correspond to the three error mechanisms discussed in the text.

error per cycle given by

$$\varepsilon_{\mathrm{sw}} \propto \exp(-t_{\mathrm{j}}/R_{\mathrm{j}}C_{\mathrm{j}}). \quad (1)$$

2. *Thermally activated tunneling.* As represented by the series of short arrows leading from island to island in figure 3, an electron can tunnel from the far end of the pump over the barrier ΔE in a series of 6 sequential events. This causes an error per cycle of

$$\varepsilon_{\mathrm{th}} \propto \exp(-\Delta E/kT), \quad (2)$$

where k is the Boltzmann constant and T is the temperature.

3. *Cotunneling.* The long solid arrow in figure 3 represents simultaneous tunneling through 6 junctions. This process, in which the intermediate states are occupied only virtually, is known as cotunneling [17]. It causes an error per cycle of

$$\varepsilon_{\mathrm{ct}} \propto \left(\frac{R_{\mathrm{K}}}{R_{\mathrm{j}}}\right)^{N-1} \left(\frac{\delta E}{\Delta E}\right)^{2N-1}, \quad (3)$$

where N is the number of junctions in the pump, R_{K} is the von Klitzing constant h/e^2, and δE is the energy range of available final states.

The expressions above are for simplified cases, but they illustrate the dependence of each error mechanism on key parameters of the pump (more accurate expressions are given in [18]). One can use these to quickly sketch the requirements for a pump that has a given error rate. For these estimates I assume the total error per cycle must be less than 10^{-8}, so I require that each individual error rate be $\sim 10^{-9}$.

1. To reach $\varepsilon_{\rm th} = 10^{-9}$ requires $\Delta E/kT \approx 20$. ΔE is simply the charging energy of a capacitor, $e^2/2C$, so the effective capacitance C should be as small as possible. For Al junctions using the fabrication technique described in section 3, the minimum C is about 0.2 fF. This implies a maximum $\Delta E/k$ of about 5 K, which means T must be less than about 25 mK. This immediately explains why conventional SET pumps used for metrology require electron-beam lithography and dilution refrigerator temperatures.
2. In the expression for $\varepsilon_{\rm sw}$, $C_{\rm j}$ is set by lithography at 0.2 fF, and $R_{\rm j}$ must satisfy the condition common to all SET devices, $R_{\rm j} \gg h/e^2 \approx 26\,{\rm k}\Omega$ [19]. Taking $R_{\rm j} = 100\,{\rm k}\Omega$ gives $R_{\rm j}C_{\rm j} =$ 0.02 ns. Since $\varepsilon_{\rm sw} = 10^{-9}$ requires $t_{\rm j}/R_{\rm j}C_{\rm j} \approx 20$, $t_{\rm j}$ must be greater than about 0.4 ns. A complete transfer cycle takes a time $Nt_{\rm j}$, and taking $N = 5$ (see next item) this time is about 2 ns. Thus the maximum current the pump can deliver without significant switching errors (from failure to tunnel during the time $t_{\rm j}$) is about $e/(2\,{\rm ns}) = 80\,{\rm pA}$.
3. Cotunneling errors set a limit on the number of junctions. For the parameters already estimated and the pulse sequence illustrated in figure 2 (which determines δE) this implies $N \geq 5$ [18].

In practice, SET pump errors do not agree quantitatively with the simple expressions given above [8,10]. However, the conclusion that counting electrons with metrological accuracy requires (1) several junctions of a size near the limits of electron-beam lithography, (2) temperatures below 0.1 K, and (3) obeying a speed limit corresponding to a current of order 10 pA, is generally valid for pumps based on Al junctions.

3 Fabricating an SET pump

The nanoscale Al tunnel junctions required by an SET pump can be fabricated using a common process involving evaporation of Al at two angles, with oxidation between layers, followed by liftoff [20]. One dimension of the junction is defined by the overlap between the two layers, and this can be controlled by adjusting the angle between the two evaporations. The current NIST recipe involves a fused quartz substrate and a bilayer resist that allows independent optimization of the develop step for the imaging and undercut layers [21]. The insulating substrate requires that the resist be coated with a thin conducting layer to prevent charging of the chip during exposure with a 30 kV electron beam. A 10 nm layer of Al, deposited by electron-gun evaporation and stripped in a solution of NaOH before the develop step, accomplishes this with little change to the required dose.

Chips with developed resist are placed in a vacuum chamber with an electron-gun evaporation source and a continuously tiltable stage. At NIST a new chamber dedicated to two-angle Al junctions has been used since early 2007, and the step where Al was evaporated with the shutter closed in the presence of O_2 [16] is no longer part of the recipe. There is less rapid aging than was seen in the old chamber when this step was not included. The first Al layer is evaporated at an angle of about 10° from normal, then the chip is oxidized in ≈ 26 Pa (200 mtorr) of O_2 for ≈ 600 s, the O_2 is pumped away, and the second Al layer is evaporated at an angle of about $-10°$. After liftoff, the completed chip is measured at a probe station with precautions against static discharge including grounding of the operator, a battery-powered multimeter, and a resistance of 1 MΩ in series with the device during measurement.

Scanning electron microscope images of completed devices are shown in figure 4. Because of the insulating substrate, the devices were coated with 10 nm of AuPd before imaging. Photos of the central region of a completed chip are shown in figure 5. The chip shown here includes an integrated SET transistor and a contact for a cryogenic needle switch, which are used to measure pump errors as described in section 6.

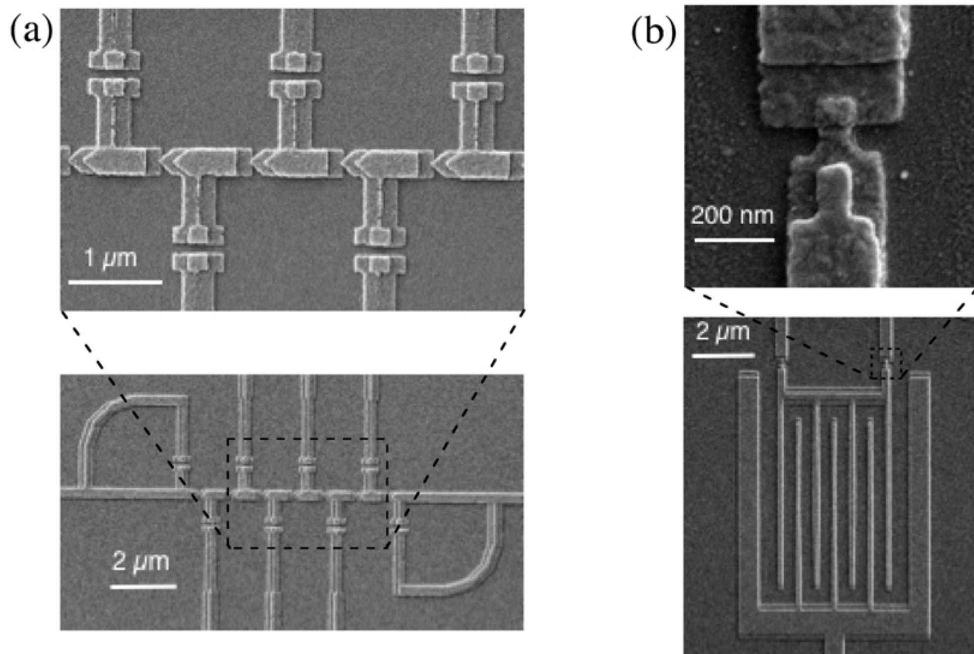

Fig. 4. Scanning electron microscope images of (a) a 7-junction SET pump and (b) an SET transistor with interdigitated gate having a capacitance of about 0.8 fF.

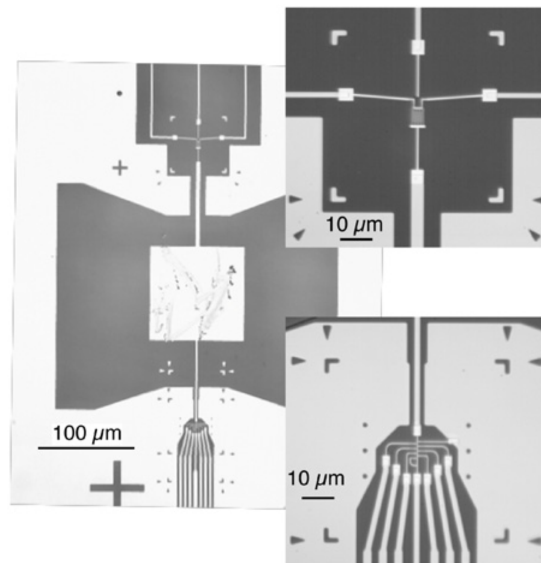

Fig. 5. Photographs of the center region of a chip containing an SET pump and transistor, as well as a landing pad for a cryogenic needle switch. Light areas are metal and dark areas are the quartz substrate. The scratches on the landing pad are caused by a probe station tip, not the needle switch.

Although none of the individual steps in this process is particularly difficult, the need to make several junctions with good uniformity, and the susceptiblity of the devices to static damage (among other failure mechanisms), make SET pump fabrication rather challenging. When the NIST process is working well, about 20% of exposed chips are worth testing at low temperature.

4 Creating a safe environment for an SET pump

Tunneling rates in SET devices depend not only on the parameters of the junction itself, but also on the electromagnetic environment surrounding the junction [19]. The theory of this effect can be used to calculate the characteristics that the environment must have to enable a pump with known parameters to achieve a specified error rate, as explained in detail in [22, 23]. These calculations show that the electrical leads to the pump, which necessarily extend to room temperature and thus carry at least the electromagnetic noise of a 300 K blackbody, must be extremely well filtered. For a typical SET pump, the filters must provide an attenuation ∼100 dB, starting at $f \sim 1$ GHz and extending to $f \sim 6$ THz (kT/h for $T \sim 300$ K). Filters made from discrete components invariably have geometrical resonances somewhere in this range [24]; thus a variety of filter designs with distributed lossy elements have been developed. The current state of the art, which includes quantitative comparisons with simulations and filters with a characteristic impedance of 50 Ω, is described in [25, 26] and in the article by D.C. Glattli in this book.

The NIST experiments currently use a modified commercial filter, developed by D.R. Schmidt and S. Allman, at both 4 K and the device temperature.The starting component is a Mini-Circuits VLFX-650 [27] 3-section low-pass filter with SMA connectors. A hole is milled in the casing of each section and a mixture of copper power (≈ 10 μm spheres) and epoxy is poured into the hole. Each filter gives about 50 dB of attenuation above 2 GHz. These filters provide moderate attenuation without distorting the pulses used to drive the pump gates, something that is not always achievable with filters having a coil of wire in a tube filled with powder and epoxy. For filters used below 0.1 K, it is important to note that stainless steel powder is not a good choice because of an anomaly in its specific heat that causes slow thermalization at these temperatures [28].

In addition to filtering the leads, the pump should be placed in an rf-shielded box so that 4 K blackbody radiation from the vacuum can surrounding the box does not reach the pump. An area inside the box can be coated with the powder and epoxy mixture to damp any radiation that enters despite the shielding and filtering.

5 Operating an SET pump

The electronics that drive the gates of the pump must provide both a dc bias and a pulse for each gate. In order that the voltage from each channel of the electronics can be treated as corresponding to a charge polarization on a single island of the pump, the effects of cross capacitance in the pump must be cancelled. The situation is illustrated in figure 6. For a voltage V_n that is intended to polarize only island n of the pump, some adjustable fraction $V' = -\beta V_n$ must be applied to each neighboring island to cancel the polarization due to cross capacitance. Furthermore, it is convenient to use one common pulse amplitude for all gates, but the gate structures in figure 1 are not all identical due to imperfect lithography, so an adjustable gain on the direct coupling is needed as well. Full cancellation for an arbitrary set of voltages $\{V_n\}$ requires a circuit like that shown in figure 6 for each of the $M = N - 1$ channels. Thus the electronics must implement an M-by-M matrix transformation between $\{V_n\}$ and $\{V'_n\}$.

All pumps measured at NIST to date have been operated using custom electronics, designed primarily by J.M. Martinis, that have 6 channels and perform the cross capacitance cancellation using a set of 36 potentiometers. The most recent incarnation uses commercial sources for the dc biases so that these may be controlled by software, has a serial interface so that the parameters for pulses of various heights can be stored and loaded from software, allows pumping to be started and stopped with an external trigger, and has fiber optic outputs that can be used to control the feedback circuit used in NIST's electron counting capacitance standard.

The main limitation of NIST's current electronics is the fact that they can generate only one type of waveform, the triangle pulses shown in figure 2. A pair of commercial 4-channel DAC boards with an update rate of 300 MHz and appropriate synchronization features has recently been programmed for pump operation by J.A. Aumentado. This will allow arbitrary waveforms for driving the pump and a software implementation of cross capacitance cancellation.

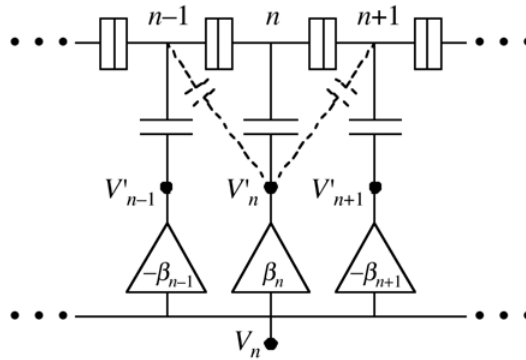

Fig. 6. Schematic of cross capacitance cancellation for island n in a pump with $M = N - 1$ gates. Capacitors in solid lines represent the direct capacitances of the gate structures in figure 1. Capacitors in dotted lines represent cross capacitances, which are shown only for nearest neighbors but are typically significant for other islands as well. For a signal intended to polarize only island n, there are M variable gains β, positive for the direct channel and negative for the cross channels, that can be adjusted to cancel the polarizations induced on neighboring islands. When the cross capacitance is properly cancelled, a voltage V_n is transformed into a set of M voltages $\{V_n'\}$ that affects only island n.

Given a chip with a working SET pump, cooled in a cryostat with good filtering and connected to the electronics just described, there are two adjustments needed to count electrons with metrological accuracy.

1. *Cross capacitance cancellation matrix.* This adjustment relies on the fact that the current-voltage curve of the pump is fundamentally periodic in the polarization charge on any island. Thus when the matrix is properly adjusted, sweeping a single V_n produces a periodic modulation, as shown in figure 7b. A detailed algorithm for adjusting the cross capacitance matrix is given in the Appendix. This process is needed only once for each device, because the cross capacitances are determined by the on-chip geometry and do not change with thermal cycling.
2. *dc bias on each gate.* Background charges in the vicinity of the junctions and islands create random island polarizations that fluctuate in time, and the dc biases must be adjusted so that the net island polarization in the absence of a pulse is much less than e. This can be done by measuring the error rate (as described in section 6) as a function of each dc bias. A given bias is swept in one direction to a threshold where the error rate increases noticeably (typically the threshold is fairly abrupt), then swept in the opposite direction until the error again increases; then the mean of the two thresholds is taken as the optimal setting for that gate. Manual adjustment of all 6 gates for a 7-junction pump, with the errors displayed on an oscilloscope, takes about 10 minutes. Starting from random values of the dc biases, two or three iterations are needed to converge on the optimal settings, after which the repeatability of the adjustment is about $\pm 0.05e$ on each island. This process must be repeated whenever any of the background charges changes by more than about $0.1e$. For the NIST 7-junction pumps, this typically occurs a few times a day immediately after cooldown and about once a day after the device has been cold for a few days.

Automated adjustment of both the cross capacitance and the dc biases is desirable if SET pumps are to be used outside a purely research environment. Limited experience at NIST indicates that these tasks can be automated, but doing them more quickly than can be done manually will likely require faster error measurements than can be obtained with a conventional SET transistor. Integrating an rf-SET transistor [29] with a pump is a promising approach, although it is not yet known whether this will affect the error rate of the pump.

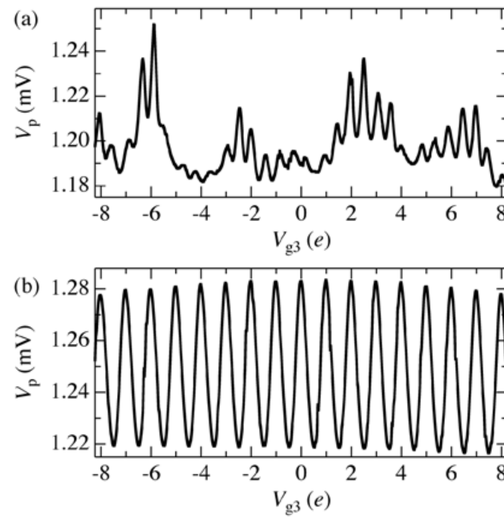

Fig. 7. Pump voltage V_p *vs.* V_g3 at constant current bias. (a) Without cross capacitance cancellation. (b) With cross capacitance cancellation properly adjusted.

6 Measuring SET pump errors

An absolute measurement of the current produced by an SET pump can be done with commercial instruments at an uncertainty $\sim 10^{-4}$ [13,30]. Reaching uncertainties below 10^{-6} for a direct measurement of a current ~ 1 pA is a significant challenge, and for most research groups it would be as difficult as making and operating the pump itself. Fortunately, there is another way to measure how often errors occur in a pump. Known as a shuttle error measurement, it involves pumping individual electrons onto an island external to the pump and detecting them with an SET transistor, as illustrated in figure 8. The circuit includes a needle switch that can be opened and closed at low temperature. Photographs of the chip and the needle switch are shown in figure 9.

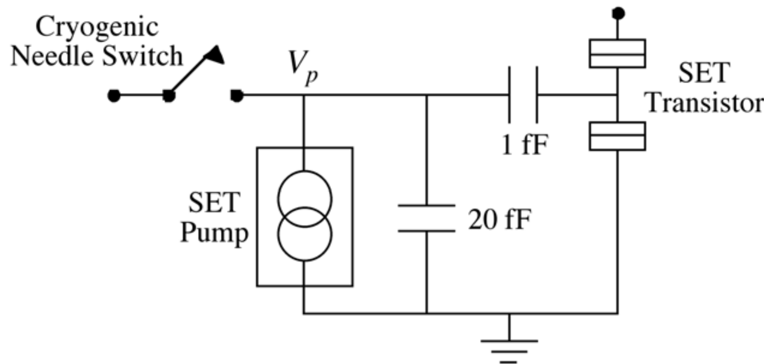

Fig. 8. Circuit for shuttle error measurement of an SET pump. An SET transistor is fabricated on the same chip as the pump, coupled by a relatively large capacitance of about 1 fF (this is the interdigitated structure shown in figure 4b). The island between the pump and transistor serves as the contact pad for a cryogenic needle switch (see figure 5) and contributes a capacitance to ground of about 20 fF.

When the needle switch is closed, one can measure the current-voltage curve of the pump, tune the cross capacitance as described in section 5, and measure the noise and gain of the transistor. When the switch is open, the transistor can easily detect individual electrons transfered by the pump, as shown in figure 10. The bandwidth of the conventional SET transistor is

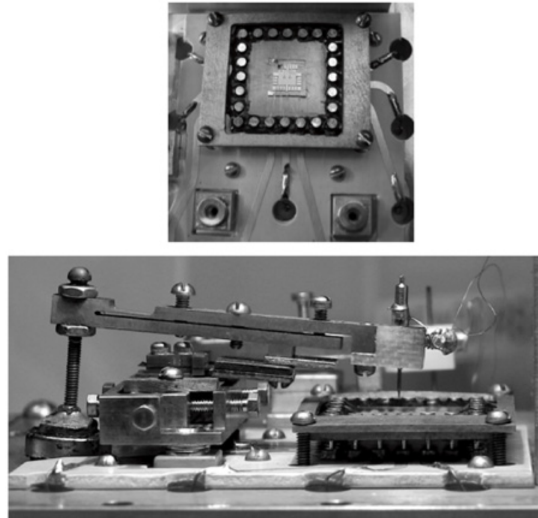

Fig. 9. Photographs of components for the shuttle error measurement. (Top) Top view of chip mounted on a header that is held down by a square brass ring. The header plugs into sockets mounted in a printed circuit board, and traces connect the sockets to coaxial connectors on the bottom of the box (not visible). The two square posts near the lower edge are where the needle switch attaches to the sample box. (Bottom) Side view of needle switch.

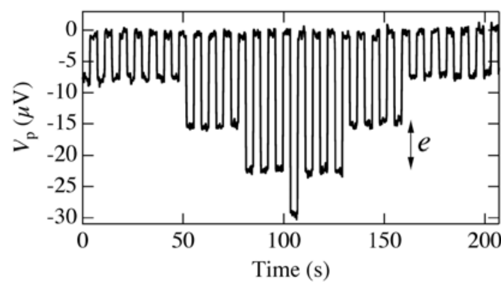

Fig. 10. SET transistor signal, converted into pump voltage V_p, *vs.* time during slow shuttle pumping of 1, 2, 3, and 4 electrons.

only $\sim 10^3$ Hz [29], so measuring every cycle and looking for mistakes that occur less than once every 10^6 cycles is not practical. However, if the pump is operated in the $\pm e$ shuttle mode at $\sim 10^6$ Hz, then perfect pumping produces a constant transistor signal, while errors that occur at $\sim 10^2$ Hz or slower appear as random jumps in the transistor signal. A typical shuttle error measurement is shown in figure 11. The leakage rate when pulses are not sent to the gates can also be measured with this technique [3].

Since the SET transistor response is periodic and the gain varies with the operating point, it is usually advantageous to operate in feedback to keep the transistor at its point of maximum sensitivity. This is done by using a simple integrator circuit that sends a signal to an auxiliary gate lead near the transistor (not shown in the schematic of figure 8, nor in the SEM images of figure 4b). A description of such a feedback scheme is given in [31].

7 Open questions

For SET pumps based on Al junctions, the dependence of the error and leakage rate on various parameters such as T, t_j, and V_p has been measured and compared with theory in several papers already cited. I will not review these studies in detail, but I will point out some areas ripe for further investigation.

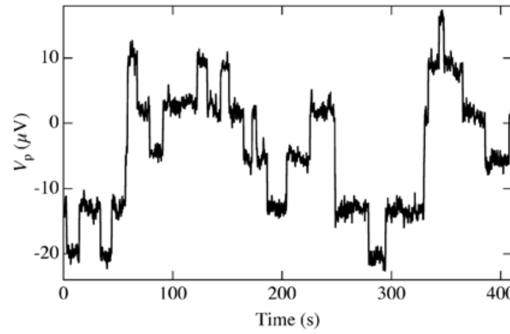

Fig. 11. V_p *vs.* time during shuttle pumping of $\pm e$ at 2.5 MHz for the 7-junction pump used in [11]. There are 32 errors in 410 s, giving an error per cycle of 3.1×10^{-8}.

1. *Identifying the error mechanism.* Comparison of theory and experiment for a 7-junction pump showed that the error and leakage rate were both orders of magnitude higher than predicted by theory [7,8]. The most obvious thing missing from the theory is photon-assisted tunneling. Adding this effect with a $1/f$ photon spectrum extending to microwave frequencies allows one to obtain good agreement with experiment, for a level of $1/f$ noise that is consistent with that measured in SET transistors at audio frequencies [10]. However, the physical source of the photons is an important open question, and the hypothesis that they come from the relaxation of charged defects [10] has not been tested. One approach would be to search for a correlation between the level of transistor noise and the error or leakage rate in a co-fabricated pump. This requires a method for controlling the transistor noise, something that has not yet been demonstrated.
2. *Reducing errors by optimizing the gate pulses.* The signals used to drive the gates of the pump determine a trajectory in the M-dimensional space defined by the gate charges. The only signals used to date are sine waves (circular trajectory for $M = 2$) and triangle waves (triangular trajectory for $M = 2$). Many more trajectories can be explored with the modern DAC cards mentioned in section 5, in particular those for which the signal is not the same for all gates. Numerical simulations of a 7-junction pump with triangle gate pulses indicate that errors are dominated by a specific part of the pumping cycle [10], which gives some guidance as to which trajectories are likely to improve performance. Another approach would be to calculate error rates for many points in the M-dimensional space and then design trajectories that pass quickly through regions where errors are most likely. The waveform described in [32] may also provide useful insight, even though it was not optimized for pumps with photon-assisted tunneling and cannot be implemented in its idealized step-like form.
3. *Maximizing the current.* All metrological applications of electron counting would benefit from higher current, so the motivation for improvements in this area is high. A true optimization of an Al junction pump for speed has not been attempted, and modest improvements may be possible by reducing the junction resistance while keeping the capacitance constant. The error measured in 7-junction pumps increases well before the speed predicted by the switching error mechanism described in section 2 (even for a more sophisticated model including heating due to pumping [10]), so the mechanism that limits pumping speed is still unknown.

8 Conclusion

While pumps based on Al junctions have demonstrated electron counting with metrological accuracy, they are not yet ready to join Josephson voltage standards, quantum Hall resistance standards and cryogenic current comparators as widely adopted items in the modern toolbox of fundamental electrical metrology. In terms of ease of fabrication, ease of operation, and

understanding of basic limitations they lag behind even more specialized tools such as ac/dc resistors, quadrature bridges, and calculable capacitors. However, a current based on e remains crucial to fundamental tests such as the quantum metrology triangle [33, 34] and related experiments [35], so various national measurement institutes will continue to develop SET devices of various types for the foreseeable future. It seems likely that one or more of the various approaches to a counted-electron current will eventually demonstrate metrological accuracy for currents much larger than 10 pA. This would enable quantum metrology triangle experiments to reach the uncertainties required to test the exactness of the Josephson voltage standard [36]. If these devices are also relatively easy to fabricate and convenient to use, they could open up new applications such as improved calibrations of currents below ∼1nA.

The contributions of the following colleagues to NIST's research on SET pumps are warmly acknowledged: Joe Aumentado, Mark Covington, Ali Eichenberger, Xavier Jehl, Dick Kautz, John Martinis, and Neil Zimmerman.

A Adjustment of cross capacitance cancellation

The following algorithm is used with the NIST custom electronics where all adjustments are performed manually, and where the pulses and dc biases are generated by circuits that are separate from the circuit that does the M-by-M matrix transformation. A similar algorithm can be used with the DAC cards where one circuit generates both pulses and dc biases, and the matrix transformation is implemented in software.

1. The pump is biased with a constant current and the pump voltage V_p is sent to the Y channel of an oscilloscope. (Biasing with a constant voltage and measuring the pump current works as well.) Recall the fundamental property of the pump current-voltage curve: it is periodic in the charge on any island, and thus changing any island charge (or any set of island charges) by an integer multiple of e will leave the current-voltage curve unchanged.
2. The pots of the Cross Capacitance Cancellation circuit can, in principle, be initialized so that the circuit performs an identity transformation, *i.e.*, no cancellation of cross capacitance. However, the tuning process converges more quickly if the initial settings correspond approximately to the cancellation required by the pump geometry.
3. The Cross Capacitance Cancellation circuit has two sets of inputs, one for pulses and one for dc biases, that are summed together before going through the matrix transformation. Disconnect the pulse and dc bias circuits from both sets of inputs.
4. Connect one set of inputs to a single function generator so that all gates can be swept together by a voltage $V_\mathrm{g,all}$, and send this voltage to the X channel of the 'scope. Set the sweep frequency to about 10 Hz. Adjust the sweep amplitude (and, if necessary, the pump bias current) so that the 'scope displays four or five quasi-periodic features, somewhat similar to those in the upper plot in figure 7. The idea here is to sweep over a significant part of the M-dimensional gate space so that the validity of the cross capacitance cancellation is not restricted to only a small part of this space.
5. Connect the other set of inputs to the outputs of the Cross Capacitance Tuner circuit. The tuner circuit generates a square wave that switches between 0 and V_sq at $f_\mathrm{sq} \approx 100$Hz, and it applies an (inverted) adjustable fraction of this square wave to each gate. The idea is that if (a) the cancellation circuit is adjusted properly and (b) the square wave amplitude corresponds to a charge of e, the set of features displayed on the scope will show nothing at the frequency f_sq because the square wave will simply switch the pump between identical current-voltage curves. If either (a) or (b) is false, a modulation at f_sq will be superimposed on the quasiperiodic features on the 'scope.
6. Choose a single value of gate voltage V_e that will correspond to a charge of e for all gates.
7. The Cross Capacitance Tuner circuit is used to tune one gate at a time, here denoted gate n, as follows:
   - Send the full square wave amplitude V_sq to gate n.

- Send a variable fraction of $V_{\rm sq}$ to the other gates. These fractions are initially set at 0 and are adjusted using a pot for each gate $m \neq n$.
- Adjust $V_{\rm sq}$ to be pe, with p an integer, for gate n. (A value of $p = 1$ is good for initial tuning, but $p = 3$ or $p = 4$ makes the tuning more sensitive to small cross capacitances.) Since the actual capacitance for gate n is not known accurately, this is done empirically: As $V_{\rm sq}$ is increased from 0, the amount of square wave will increase and decrease periodically, with the minima corresponding to multiples of e.
- Tune the pots for gates $m \neq n$ of the Cross Capacitance Tuner circuit to minimize the square wave visible on the scope. (Note that these are separate pots from those in the Cross Capacitance *Cancellation* circuit. The reason for two sets of pots in NIST's custom electronics is that those in the Tuner circuit are large and easy turn by hand, while those in the Cancellation circuit must be small for good high frequency performance and require a small screwdriver for turning.) It is better to optimize several features than to cancel the square wave perfectly on a single feature. Iterate the adjustment until it cannot be improved.
- The pots of the Tuner circuit are now performing the desired cancellation for gate n, and this effect must be transferred to the pots of the Cancellation circuit, as described next.
  - Turn off the sweep of $V_{\rm g,all}$ from the function generator.
  - Set the square wave to its high value ($V_{\rm sq}$ corresponding to pe).
  - Record the voltages $\{V'_n\}$ coming out of the cancellation circuit for all gates. Recall that these voltages are produced for an input pe on the *actual* gate capacitance of gate n.
  - Set the Tuner circuit so that the fractions for all gates $m \neq n$ are 0.
  - Set $V_{\rm sq}$ to pV_e.
  - Tune the pots of the Cancellation circuit corresponding to gate n (that is, the nth row of the M-by-M matrix) in order to obtain the voltages $\{V'_n\}$ recorded above. The Cancellation circuit is now producing the same effect as the Tuner circuit was producing before, and it is doing so for an input that is p times the common value chosen above. This means that the direct coupling for gate n has also been adjusted so that an input of V_e corresponds to a charge of e on island n.

8. The cancellation can be checked by sweeping a single V_n, which should produce a modulation on the scope with a single period equal to V_e, similar to figure 7b.

References

1. H. Pothier, P. Lafarge, C. Urbina, D. Esteve, M.H. Devoret, Europhys. Lett. **17**, 249 (1992)
2. J.M. Martinis, M. Nahum, H.D. Jensen, Phys. Rev. Lett. **72**, 904 (1994)
3. M.W. Keller, J.M. Martinis, N.M. Zimmerman, A.H. Steinbach, Appl. Phys. Lett. **69**, 1804 (1996)
4. E.R. Williams, R.N. Ghosh, J.M. Martinis, J. Res. Natl. Inst. Stand. Technol. **97**, 299 (1992)
5. M.W. Keller, A.L. Eichenberger, J.M. Martinis, N.M. Zimmerman, Science **285**, 1706 (1999)
6. M.W. Keller, N.M. Zimmerman, A.L. Eichenberger, Metrologia **44**, 505 (2007)
7. M.W. Keller, J.M. Martinis, R.L. Kautz, Phys. Rev. Lett. **80**, 4530 (1998)
8. R.L. Kautz, M.W. Keller, J.M. Martinis, Phys. Rev. B **60**, 8199 (1999)
9. M. Covington, M.W. Keller, R.L. Kautz, J.M. Martinis, Phys. Rev. Lett. **84**, 5192 (2000)
10. R.L. Kautz, M.W. Keller, J.M. Martinis, Phys. Rev. B **62**, 15888 (2000)
11. X. Jehl, M.W. Keller, R.L. Kautz, J. Aumentado, J.M. Martinis, Phys. Rev. B **67**, 165331 (2003)
12. A.B. Zorin, S.V. Lotkhov, H. Zangerle, J. Niemeyer, J. Appl. Phys. **88**, 2665 (2000)
13. H. Scherer, S.V. Lotkhov, G.-D. Willenberg, A.B. Zorin, IEEE Trans. Instrum. Meas. **54**, 666 (2005)
14. M.W. Keller, *Recent Advances in Metrology and Fundamental Constants*, edited by T.J. Quinn, S. Leschiutta, P. Tavella, Volume CXLVI of *Proceedings of International School of Physics "Enrico Fermi"* (Amsterdam, IOS Press, 2001), p. 291
15. A. Kemppinen, M. Meschke, M. Möttönen, D.V. Averin, J.P. Pekola, Eur. Phys. J. Special Topics **172**, 311 (2009)

16. M.W. Keller, J.M. Martinis, A.H. Steinbach, N.M. Zimmerman, IEEE Trans. Instrum. Meas. **46**, 307 (1997)
17. D.V. Averin, Yu.V. Nazarov, *Single Charge Tunneling: Coulomb Blockade Phenomena in Nanostructures*, edited by H. Grabert, M.H. Devoret (Plenum Press, New York, 1992), p. 217
18. H.D. Jensen, J.M. Martinis, Phys. Rev. B **46**, 13407 (1992)
19. M.H. Devoret, H. Grabert, *Single Charge Tunneling: Coulomb Blockade Phenomena in Nanostructures*, edited by H. Grabert, M.H. Devoret (Plenum Press, New York, 1992), p. 1
20. G.J. Dolan, Appl. Phys. Lett. **31**, 337 (1977)
21. B. Cord, C. Dames, K.K. Bergren, J. Aumentado, J. Vac. Sci. Technol. B **24**, 3139 (2006)
22. J.M. Martinis, M. Nahum, Phys. Rev. B **48**, 18316 (1993)
23. D. Vion, P.F. Otfila, P. Joyez, D. Esteve, M.H. Devoret, J. Appl. Phys. **77**, 2519 (1995)
24. H. Courtois, O. Buisson, J. Chaussy, B. Pannetier, Rev. Scient. Instr. **66**, 3465 (1995)
25. H. le Sueur, P. Joyez, Rev. Scient. Instr. **77**, 115102 (2006)
26. F.P. Milliken, J.R Rozen, G.A. Keefe, R.H. Koch, Rev. Sci. Instrum. **78**, 24701 (2007)
27. The identification of specific commercial instruments does not imply endorsement by NIST nor does it imply that the instruments identified are the best available for a particular purpose
28. C. Hagmann, P.L. Richards, Cryogenics **35**, 345 (1995)
29. R.J. Schoelkopf, P. Wahlgren, A.A. Kozhevnikov, P. Delsing, D.E. Prober, Science **280**, 1238 (1998)
30. T.J.B.M. Janssen, A. Hartland, Physica B **284-288**, 1790 (2000)
31. M. Furlan, S.V. Lotkhov, Phys. Rev. B **67**, 205313 (2003)
32. L.R.C. Fonseca, A.N. Korotkov, K.K. Likharev, Appl. Phys. Lett. **69**, 1858 (1996)
33. K.K. Likharev, A.B. Zorin, J. Low Temp. Phys. **59**, 347 (1985)
34. F. Piquemal, G. Genevès, Metrologia **37**, 207 (2000)
35. M.W. Keller, F. Piquemal, N. Feltin, B. Steck, L. Devoille, Metrologia **45**, 330 (2008)
36. M.W. Keller, Metrologia **45**, 102 (2008)